3

Numerical Investigation of Disordered Patch Resonator Absorbers

3.1 INTRODUCTION

As discussed in Chapter 2, low profile, flexible, light-weight and mechanically stable wideband absorbers are required for many applications such as radome, stealth technology, photodetection, electromagnetic shielding (EMI), electromagnetic compatibility (EMC), etc. The MPAs are excellent candidates for all these applications as they are low-profile, light-weight, ultrathin, and mechanically stable structures. The earlier reported MPAs have narrow absorption bandwidth as the absorption mechanism was based on the structural resonance effect. To further enhance the absorption bandwidth, various design techniques were employed in the literature eg. multi-scale, multi-layer, lumped component loaded MPA structures. However, their applications are limited due to increased design complexity, large thickness, and high fabrication cost.

One approach to address this issue is to employ disordered metamaterial structures. As reviewed in the Chapter 2, they are less explored compared to their periodic counterparts; however, they have the potential of resolving the issue of the inherent narrow bandwidth of the MPAs, especially at higher frequency domain. In this Chapter, a disordered patch resonator-based absorber structure is proposed and analyzed numerically. Initially, a periodic circular patch-based absorber structure is presented, which was then thoroughly investigated using an equivalent electric circuit model in terms of quality factors. Instead of the popularly used RLC equivalent circuit model, the quality factor approach is used as the proposed structure is very thin, and it does not satisfy the $h/p > 0.3$ condition, where h is the substrate thickness and p is the periodicity. For thinner substrate, the values of capacitance, inductance and resistance can not be determined accurately [Costa *et al.*, 2012]. A controllable position disorder is introduced in the initial periodic structure. Then this disordered structure is analyzed for different values of the disorder parameter. Later, the effect of increasing filling factor (which is defined as the ratio of the total area occupied by the resonators and area of the entire sample) on the disordered absorber structure is investigated, followed by oblique incidences analysis. In the end, a square patch-based absorber is studied for both periodic and disordered settings.

3.2 PERIODIC CIRCULAR PATCH RESONATOR ABSORBERS

A periodic absorber with an unit cell consisting of a circular patch as shown Figure 3.1 in is designed for benchmarking. The circular metal patch of radius r is deposited on a grounded FR4 dielectric substrate ($\varepsilon_r = 4.2$, $\tan\delta = 0.02$, thickness $= 1$mm).

Treating the circular patch as a radiation patch element of a single microstrip patch antenna, the resonance frequency can be deduced by [Balanis, 2016],

$$f_r = \frac{1.8412}{2\pi r_e \sqrt{\varepsilon_r}\sqrt{\varepsilon_o \mu_o}}, \tag{3.1}$$

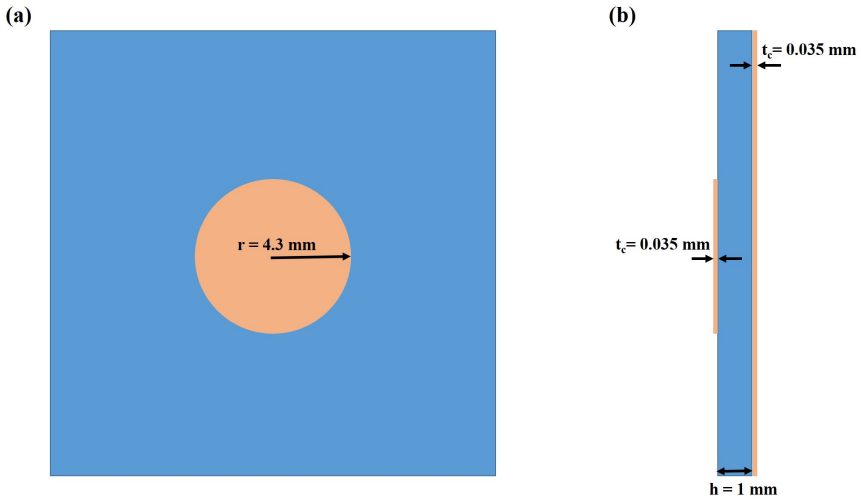

Figure 3.1 : Top and side view of the unit cell of the designed periodic circular patch absorber

where r_e is the effective patch radius and it is defined as follows

$$r_e = r\left\{1+\frac{2h}{\pi r\varepsilon_r}\left[\ln\left(\frac{\pi r}{2h}\right)+1.7726\right]\right\}^{1/2}.$$

here h is the thickness of the dielectric substrate. For $r = 4.3$ mm, we get $f_r = 9.25$ GHz from Eq. (3.1). Hence for the designed circular patch resonator of radius $r = 4.3$ mm, the resonant frequency will be at 9.25 GHz. Although the resonant frequency is obtained, still for achieving the perfect absorption condition at the resonant frequency, the optimal period is required. For deducing the optimal period, generally, time-intensive parametric numerical simulations were performed. To eliminate this step, here an equivalent electric circuit model, as shown in Figure 3.2 is studied using the quality factor approach for deducing the optimal period for perfect absorption condition.

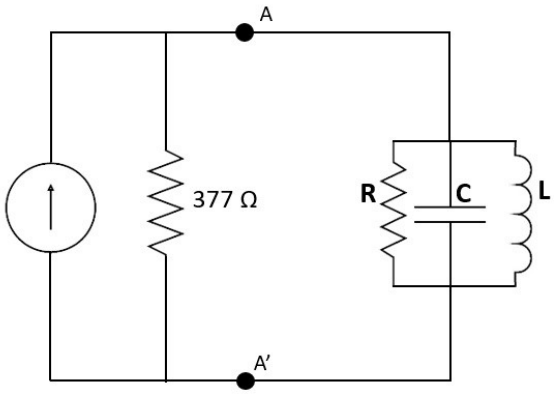

Figure 3.2 : Equivalent electrical circuit model for the periodic patch resonator absorbers.

The normal incident electromagnetic wave is modeled by free-space wave impedance (377 Ω), resistance R is provided by the losses in the absorber (ohmic and dielectric), whereas capacitance C and inductance L are determined by the periodicity and patch dimension. Three quality factors are defined based on the equivalent electrical model [Yoshiizumi *et al.*, 2015] i.e.

Q_{rad}, Q_{diss} and Q_{total} which are equivalent to unloaded Q_o, external Q_e and loaded Q_L quality factors defined in [Pozar, 2009] and given as follows

$$\frac{1}{Q_{total}} = \frac{1}{Q_{diss}} + \frac{1}{Q_{rad}}. \tag{3.2}$$

Here $Q_{diss}^{-1} = Q_c^{-1} + Q_d^{-1}$ defines the total losses occurring in the structure, where Q_c is conductance loss and Q_d is dielectric loss respectively. Q_{rad} is the radiative quality factor and it denotes a coupling between the resonating structure and the incident wave. It depends on the period of the structure.

At the resonance frequency, the loss process is primarily located in the dielectric as seen from Figure 3.3. Therefore the conductance losses are neglected. The dielectric quality factor is given as $Q_d = (\tan\delta)^{-1}$ [Bliokh *et al.*, 2008].

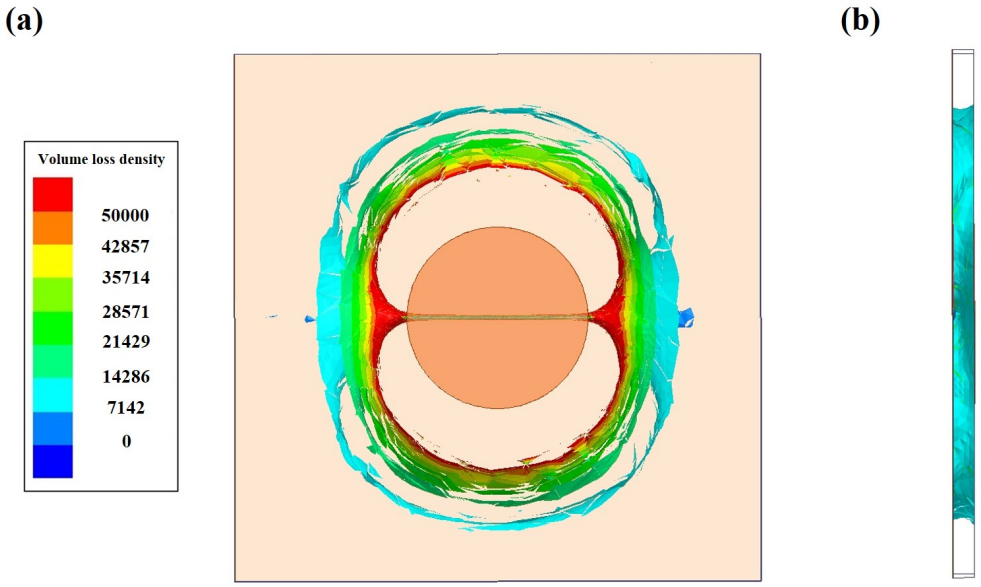

Figure 3.3 : The simulated (a) Top and (b) side view of the unit cell displaying the losses occurring in the dielectric substrate at the resonance frequency.

Hence Eq. (3.2) gets modified as

$$\frac{1}{Q_{total}} = \frac{1}{Q_d} + \frac{1}{Q_{rad}}. \tag{3.3}$$

For achieving the perfect unit absorption condition, one should have $Q_d = Q_{rad}$ [Qu *et al.*, 2015], which also corresponds to the free space impedance matching condition. Now from Eq. (3.3), for perfect absorption condition we get $Q_{total}^{-1} = 2{Q_d}^{-1}$, on putting the loss tangent $(\tan\delta = 0.02)$ value in the above equation we get $Q_{total} = 25$, which is used as the optimal period for achieving the perfect absorption at the resonant frequency [Fernez *et al.*, 2018].

The proposed circular patch with radius $r = 4.3$ mm and periodicity $p = 25$ mm is simulated using commercial software ANSYS HFSS 2013. The simulated absorption spectrum is shown in Figure 3.4. As seen from the figure, perfect absorption condition is achieved at the resonant

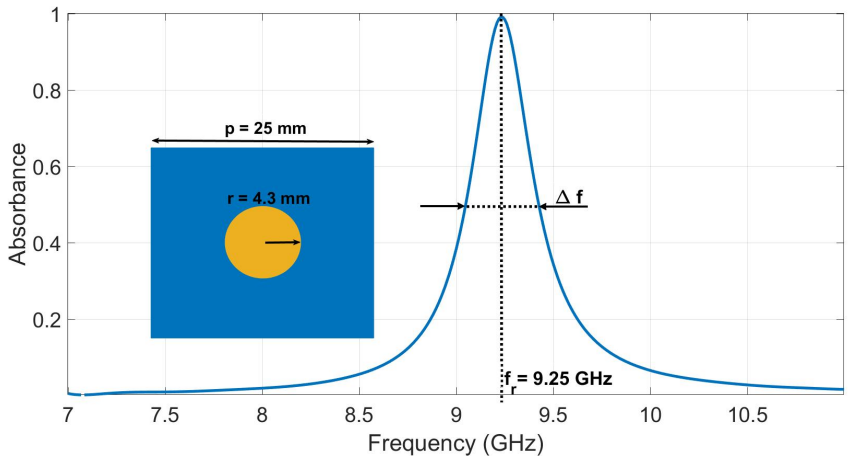

Figure 3.4 : Simulated absorption spectrum for the circular patch resonator absorber.

frequency 9.25 GHz. Further, the optimal period was also calculated by parametric optimization method. Figure 3.5 shows the absorbance versus periodicity plot, it is clearly evident that the maximum absorbance is achieved for $p = 25$ mm.

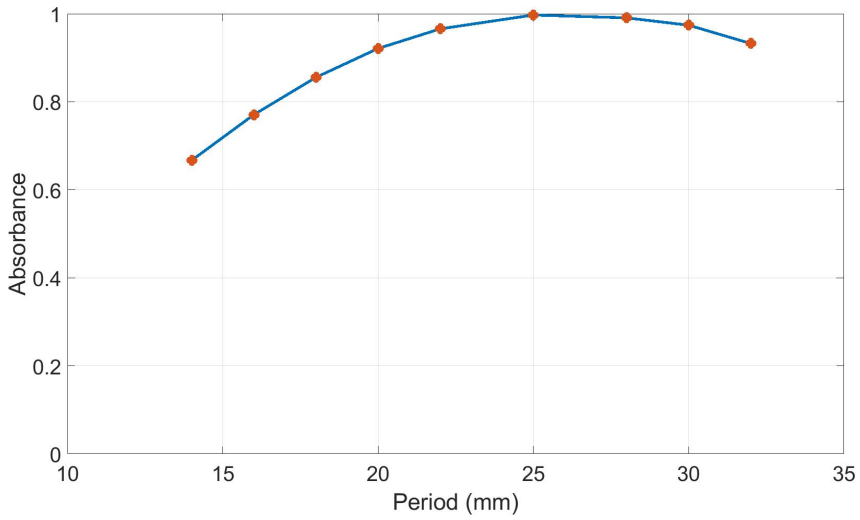

Figure 3.5 : Simulated absorbance versus periodicity for the circular patch resonator absorber.

Moreover the critical coupling condition can also be deduced from the absorption spectrum and it satisfies

$$Q_{total} = \frac{f_r}{\Delta f}, \tag{3.4}$$

where f_r = resonance frequency and Δf = full-width half maximum around the resonance frequency as shown in Figure 3.4.

From Figure 3.4, putting values in Eq. (3.4) we get $Q_{total} = 25$ for the proposed circular patch absorber, which is consistent with what we get from the earlier equivalent model approach.

Surface currents along with E and H fields at the resonant frequency for the proposed circular patch absorber are plotted in Figure 3.6. As seen from the figure, at the resonant frequency the counter-propagating currents in the top metallic patch (Figure 3.6(a)) and the ground plane (Figure 3.6(b)) along with the displacement current (due to out of plane E-field) give rise to an in-plane magnetic dipole. In the periodic circular patch absorber, when the structure is excited by the incident electromagnetic wave, all the resultant magnetic dipoles are oriented in the same direction resulting in a degenerated frequency response. This degeneracy, however, will be lifted in the disordered structure due to the different orientation and alignment of the resultant magnetic dipoles resulting in significant interaction among the neighboring resonators. Such disordered structures are analyzed in the next section.

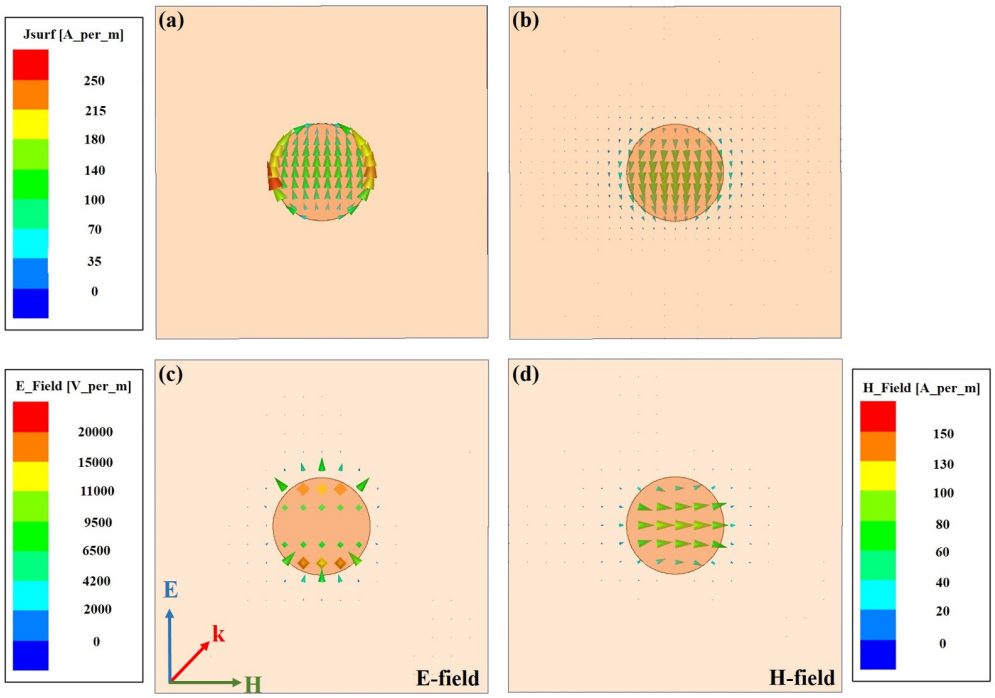

Figure 3.6 : (a,b) Anti-parallel surface currents on the top and ground metallic plane (c,d) are E-field and H-field maps at the resonance frequency plotted in dielectric mid plane.

3.3 DISORDERED PATCH ABSORBER STRUCTURE

3.3.1 Effect of Position Disorder

Following a common approach, the position disorder was introduced into the initial periodic setting by displacing each circular patch resonator from its original position by adding an uniform spatial disorder, which was randomly selected from the interval

$$\Delta x, \Delta y \in \left[\frac{-D.p}{2}, \frac{D.p}{2}\right] \tag{3.5}$$

where D is a dimensionless disorder parameter and p is the periodicity of initial periodic structure [Helgert *et al.*, 2009]. Three different structures as shown in Figure 3.7(b) were simulated for no positional disorder ($D = 0$), moderate positional disorder ($D = 0.5$), and high positional disorder ($D = 1$).

The simulation of disordered/random media is computationally extensive task both in

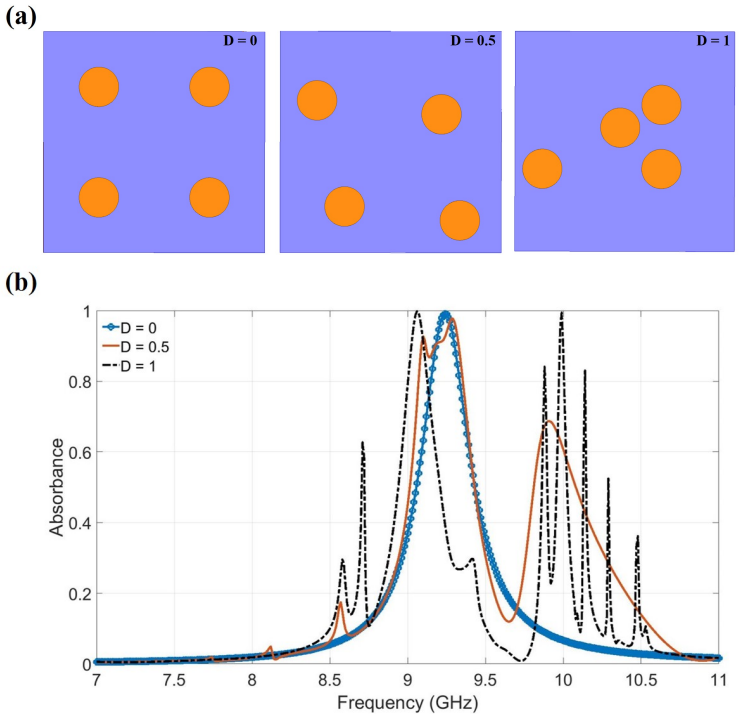

Figure 3.7 : (a) Disordered structures corresponding to three different disorder parameters, (b) Absorption spectrum for three different disorder structures.

terms of memory and time requirement, therefore supercell approach was used for the numerical simulations of disordered structure. The patch resonators were randomly positioned in a supercell (50 x 50 mm^2) by displacing the initial periodic centres by adding a uniformly distributed disorder mentioned above. The supercell was than truncated in both lateral directions by electric and magnetic boundary conditions. This results in a quasi-random array i.e. a periodic array of supercells and within each supercell resonators are randomly positioned. Therefore, the term 'disorder' is used instead of 'random' throughout the Chapter.

It is evident from the Figure 3.7(a), that the effect of position disorder is negligible for a moderate degree of disorder ($D = 0.5$). The absorption spectrum is similar to that of a periodic structure ($D = 0$). However, in the case of highly disordered structure ($D = 1$), many unevenly distributed additional peaks are seen. This is due to the random distribution of the distances between the resonators resulting in various coupled resonances at different frequencies.

3.3.2 Effect of Increasing Filling Fraction

Further, the effect of increasing resonator packing density on the disordered absorber structure is analyzed. As mentioned earlier, here also the supercell approach is employed for the simulation of disordered structures. The filling fraction of the resonators in the supercell is gradually increased. The filling factor (FF) is defined as the ratio of the total area occupied by the resonators and the area of the supercell, i.e.

$$FF = \frac{N\pi r^2}{a^2}, \tag{3.6}$$

where r is the radius of the circular resonator, N is total number of resonators and a is supercell of dimension 48×48 mm^2.

Four different filling factors i.e 10%, 20%, 30% and 40% were selected. A MATLAB code was written for generating uniform randomly distributed center coordinates for the circular resonators inside the supercell. The overlapping resonator condition was excluded to remove any ambiguity in the analysis of electromagnetic coupling, thus limiting the analysis up-to 40% filling factor value. As seen in Figure 3.8, three different structures were generated per filling factor configuration.

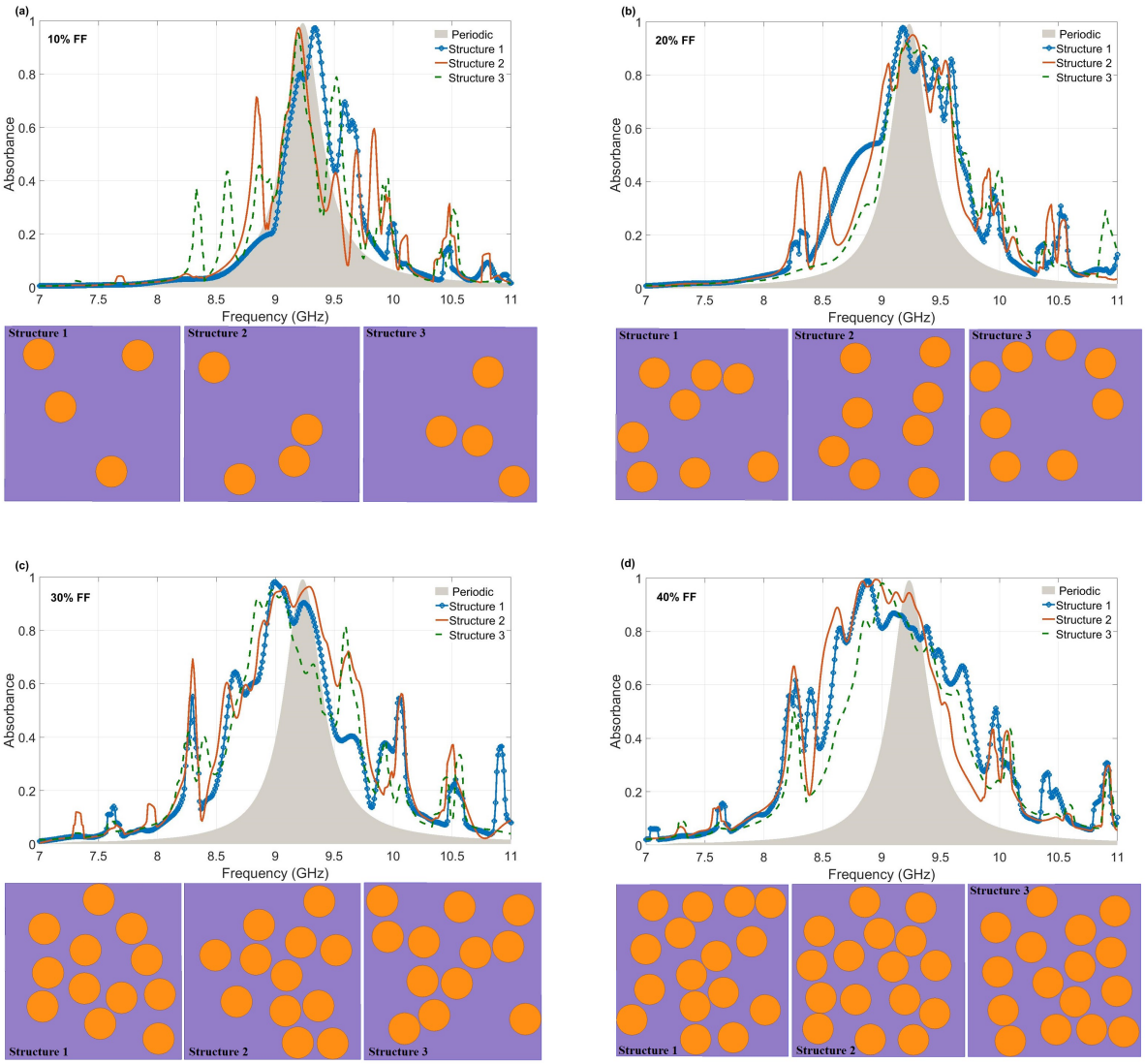

Figure 3.8 : Simulated absorption spectrum for disordered absorber: (a) 10 % FF, (b) 20 % FF, (c) 30 % FF, and (d) 40 % FF. Three different structures were simulated per filling factor configuration at normal incidence for TE polarization.

Even for low filling factor (10 % FF), additional peaks are observed near the resonance frequency of the periodic structure. As discussed earlier, these additional peaks arise due to the random distribution of distances among the resonators, resulting in coupled resonances resonating at slightly different frequencies in the vicinity of the resonant frequency, see Figure 3.8(a). When the filling factor was further increased to 40 %, the resonators were more densely packed, resulting in substantial coupling among themselves. This coupling among the nearby resonators resulted

in an inhomogeneous broadening along with a slightly decreased line width of the absorption bandwidth, as seen from Figure 3.8(d).

For higher filling factors, a redshift in absorption frequencies was observed in Figure 3.8(c,d). This redshift is due to the formation of clusters like structures that support additional lower frequency modes which were formed when the resonators were closely spaced with minimal separation among them.

The effect of coupling among the neighboring resonators was analyzed further. E-field maps at three different frequencies for 30% FF case of both the TE and TM polarization are plotted in Figure 3.9 at normal incidence. As seen from Figure 3.9, at a frequency (8 GHz) just below the resonance, there was little or no coupling among the resonators, and the resonators were weakly excited. At the resonance frequency (9 GHz), all the resonators were strongly excited, and strong coupling among the neighboring resonators can be seen. However, at higher frequency (10 GHz), only the isolated resonators were strongly excited, and no significant coupling among them was observed for both the TE and TM polarizations.

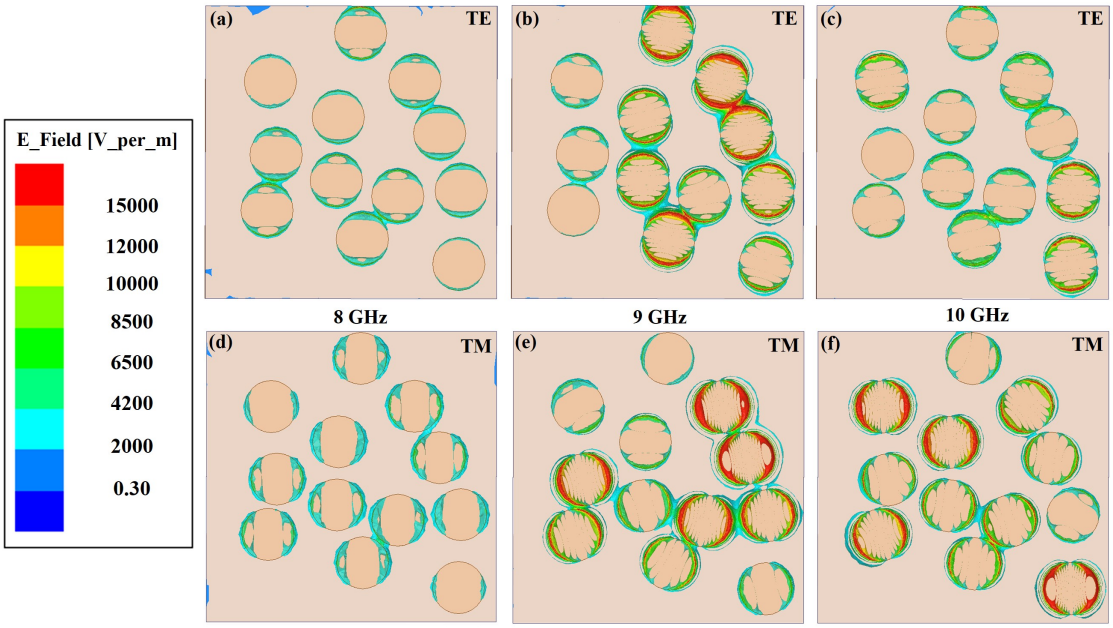

Figure 3.9 : E-field maps for the 30 % FF case (normal incidence) for both the TE and TM polarization at (a) 8 GHz, (b) 9 GHz and (c) 10 GHz.

3.3.3 Effect of Oblique Incidences

Till now, the absorption characteristics of the disordered absorber structures were explored under normal incidence condition. Here, the effect of oblique incidences on the disordered absorber structures is investigated. For this 30% filling factor case was considered. Master-slave boundary conditions were used in combination with the Floquet port for providing oblique incidences condition. Figure 3.10 shows TE and TM polarization responses for oblique incidences up-to 45^{o}. As evident from the figure, near unity absorption was achieved at the resonant frequency for both the polarizations for all incidence angles. Similarly, the overall absorption response, which depends upon the coupling among the in-plane magnetic dipoles and the magnetic field component of the incident wave was stable for the wide incidence angles for both the TE and TM polarizations. This is an encouraging response as it is difficult to achieve polarization insensitivity in the conventional periodic metamaterial structures without any special design constraint.

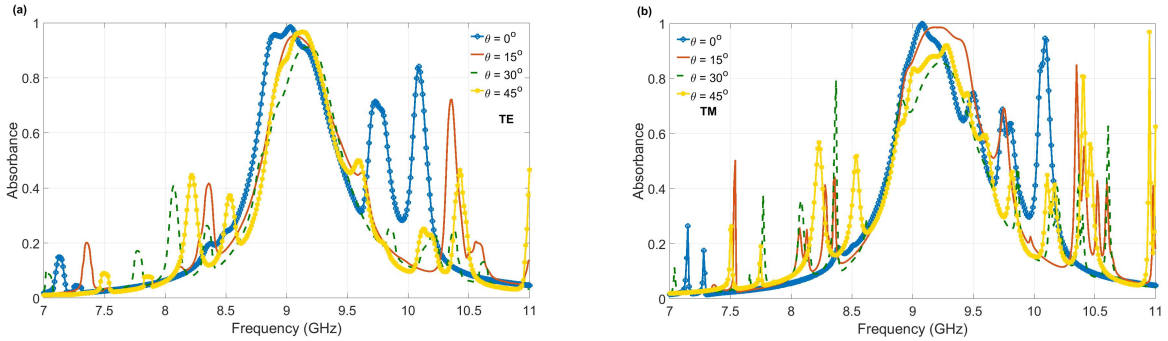

Figure 3.10 : Simulated absorption spectrum of circular patch resonator based absorber for (a) TE and (b) TM polarization for 30 % FF case for oblique incidences.

3.3.4 Effect of Patch Resonator Shape

Here the effect of patch resonator shape on the enhanced absorption characteristics of disordered resonator absorber is investigated. For this, a square patch resonator-based absorber is explored under both the periodic as well as disorder settings. The square patch is designed to have the same resonant frequency as that of the circular patch so that the direct comparison can be made. The deduced side length is $l = 7.3$ mm. As seen from Figure 3.11, the absorption spectrum of the periodic square patch absorbers is similar to that of a circular patch absorber in Figure 3.4.

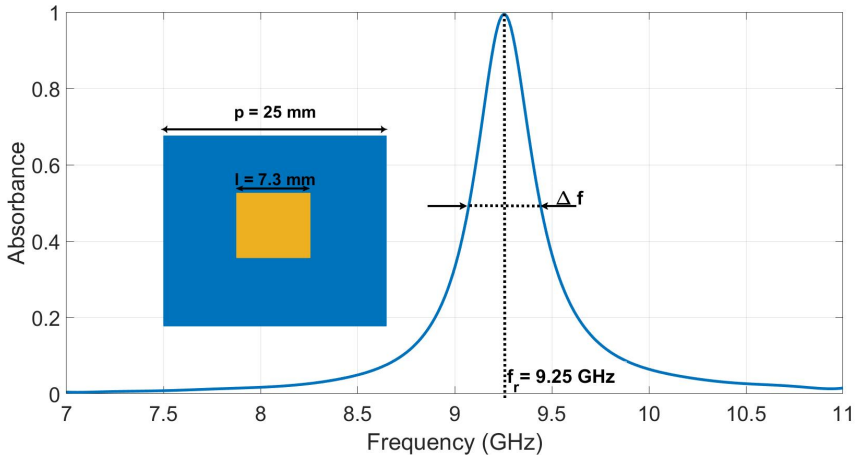

Figure 3.11 : Simulated absorption spectrum for square patch absorbers. Inset is the unit cell structure for the square patch resonator absorbers.

Moreover, similar position disorder as in the circular absorbers case was introduced in the periodic square patch absorbers. Two different filling factors were taken into account i.e 10% FF and 30%FF. Here the filling factor is defined as

$$FF = \frac{Nl^2}{a^2} \tag{3.7}$$

where N is the total number of resonators, l is the side length of the square patch and a is the supercell of dimension 48×48 mm^2.

As seen from Figure 3.12, the absorption properties of disordered square patch absorbers

were similar to that of the disordered circular patch absorbers corresponding to the same filling factor configuration. Subsequent E-field plots in Figure 3.13 have similar characteristics to that of the circular patch absorber. Significant enhancement in absorption bandwidth due to coupling among neighboring square patches was observed near the vicinity of the resonant frequency at 9 GHz. However, the resonators were weakly excited at the lower and higher frequencies.

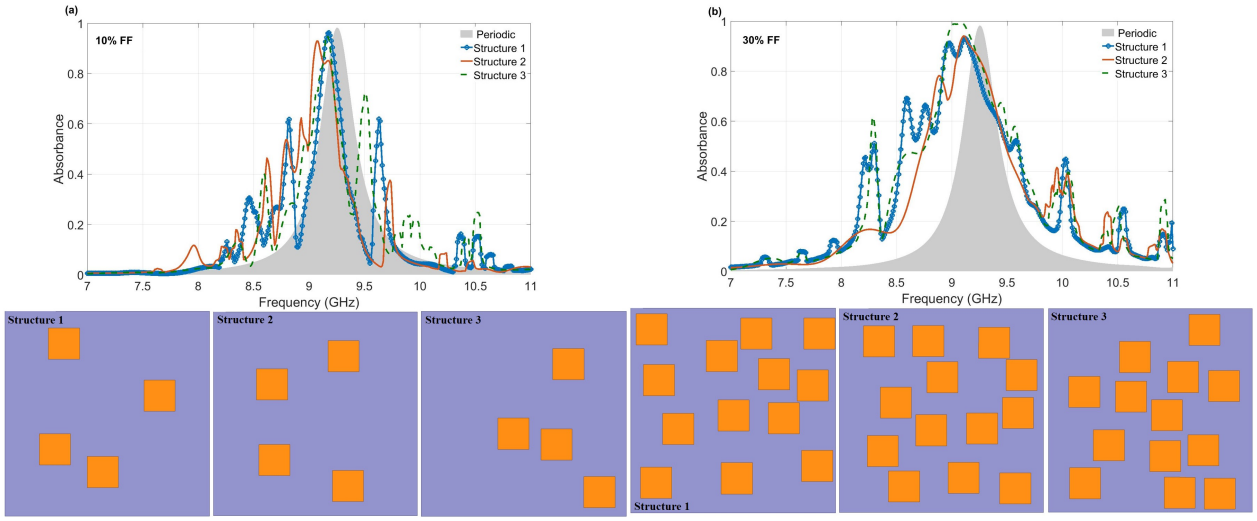

Figure 3.12 : Simulated absorption spectrum for square patch disordered absorbers: (a) 10 % FF and (b) 30 % FF. Three different structures were simulated per filling factor configuration.

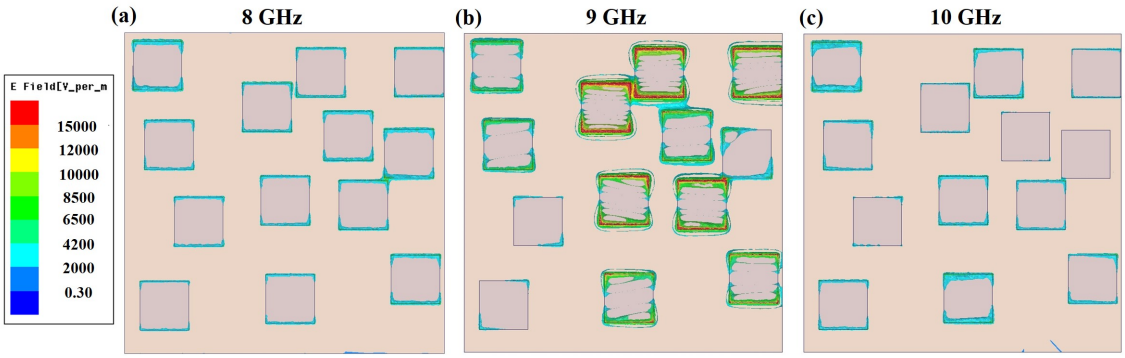

Figure 3.13 : E-field maps for the 30 % FF case (normal incidence) for TE polarization at (a) 8 GHz, (b) 9 GHz and (c) 10 GHz.

Thus it can be deduced that the bandwidth enhancement properties of the disordered structures are independent of the shape of the patch resonators and are mainly dependent upon the coupling among the neighboring resonators. Slight differences among the secondary resonances of the circular and square patches are due to the difference in the symmetry of the patch structures.

3.4 SUMMARY

In this Chapter, absorption in periodic circular patch resonator absorbers has been analyzed by the quality factor approach. To enhance the absorption bandwidth of the patch resonator absorber, position disorder was introduced in the initial periodic setting. The enhancement in the absorption bandwidth was directly related to the filling factor. More the filling factor, more densely

the resonators are packed, resulting in increased coupling among the neighboring resonators. It was numerically demonstrated that the designed disordered patch resonator absorbers were polarization-insensitive, and have stable absorption response even for oblique incidence angles for both TE and TM polarizations. Further, the square patch resonator absorbers were studied under both the periodic and disordered settings. It was observed that the enhancement in absorption bandwidth of the disordered structures was independent of the shape of the patch resonators and depends solely upon coupling among neighboring resonators.

...